
This is an electronic reprint of the original article.
This reprint may differ from the original in pagination and typographic detail.

Olszewska, Anna; Valle-Delgado, Juan José; Nikinmaa, Miika; Laine, Janne; Österberg, Monika

Direct measurements of non-ionic attraction and nanoscaled lubrication in biomimetic composites from nanofibrillated cellulose and modified carboxymethylated cellulose

Published in:
Nanoscale

DOI:
[10.1039/c3nr03091a](https://doi.org/10.1039/c3nr03091a)

Published: 01/01/2013

Document Version
Peer-reviewed accepted author manuscript, also known as Final accepted manuscript or Post-print

Please cite the original version:
Olszewska, A., Valle-Delgado, J. J., Nikinmaa, M., Laine, J., & Österberg, M. (2013). Direct measurements of non-ionic attraction and nanoscaled lubrication in biomimetic composites from nanofibrillated cellulose and modified carboxymethylated cellulose. *Nanoscale*, 5(23), 11837-11844. <https://doi.org/10.1039/c3nr03091a>

This material is protected by copyright and other intellectual property rights, and duplication or sale of all or part of any of the repository collections is not permitted, except that material may be duplicated by you for your research use or educational purposes in electronic or print form. You must obtain permission for any other use. Electronic or print copies may not be offered, whether for sale or otherwise to anyone who is not an authorised user.

Nanoscale

Accepted Manuscript

This article can be cited before page numbers have been issued, to do this please use: A. M. Olszewska, J. J. Valle-Delgado, M. Nikinmaa, J. Laine and M. Österberg, *Nanoscale*, 2013, DOI: 10.1039/C3NR03091A.



This is an *Accepted Manuscript*, which has been through the RSC Publishing peer review process and has been accepted for publication.

Accepted Manuscripts are published online shortly after acceptance, which is prior to technical editing, formatting and proof reading. This free service from RSC Publishing allows authors to make their results available to the community, in citable form, before publication of the edited article. This *Accepted Manuscript* will be replaced by the edited and formatted *Advance Article* as soon as this is available.

To cite this manuscript please use its permanent Digital Object Identifier (DOI®), which is identical for all formats of publication.

More information about *Accepted Manuscripts* can be found in the [Information for Authors](#).

Please note that technical editing may introduce minor changes to the text and/or graphics contained in the manuscript submitted by the author(s) which may alter content, and that the standard [Terms & Conditions](#) and the [ethical guidelines](#) that apply to the journal are still applicable. In no event shall the RSC be held responsible for any errors or omissions in these *Accepted Manuscript* manuscripts or any consequences arising from the use of any information contained in them.

Cite this: DOI: 10.1039/c0xx00000x

www.rsc.org/xxxxxx

ARTICLE TYPE

Direct measurements of non-ionic attraction and nanoscaled lubrication in biomimetic composites from nanofibrillated cellulose and modified carboxymethylated cellulose

Anna Olszewska,* Juan José Valle-Delgado, Miika Nikinmaa, Janne Laine, Monika Österberg*

Received (in XXX, XXX) Xth XXXXXXXXX 20XX, Accepted Xth XXXXXXXXX 20XX
DOI: 10.1039/b000000x

There is a growing interest to design biomimetic self-assembled composite films from renewable resources aimed at a combination of high toughness, strength and stiffness. However, the relationship between interfacial interactions of the components and the mechanical performance of the composite is still poorly understood. In this work we present evidence of the link between mechanical performance of carbohydrate-based composites with nanolubrication and with direct surface forces between the hard and soft domain in the system. Our approach was to use nanofibrillated cellulose (NFC) as the major reinforcing domain and to modify it by adsorption of a small amount of soft polyethylene glycol grafted carboxymethyl cellulose (CMC-g-PEG). The effect of the soft polymer on direct normal and friction forces in air between cellulose surfaces was evaluated using colloidal probe microscopy. The fibrillar structure of the NFC thin film affected the frictional behaviour; when decreasing load, the friction between pure cellulose surfaces increased, suggesting partial pull-out of fibrils, a phenomenon not observed for non-fibrillar cellulose substrates. Adsorption of CMC-g-PEG on both surfaces decreased the friction considerably but adhesion was still high. The symmetric system, having both cellulose substrates covered with polymer, was compared to asymmetric systems where only one surface was covered with polymer. Furthermore, a free standing composite film was prepared by non-ionic self-assembly of NFC and CMC-g-PEG with 99:1 weight-ratio; the mechanical properties of the macroscopic films were related to the nanoscaled interactions between the components. The composition studied showed excellent mechanical properties which do not follow the simple rule of mixture. Thus, a synergy in the direct surface forces and mechanical properties was found. This approach offers a robust path to aid in the efficient design of next generation biomimetic composites.

Introduction

There is a strong interest to design low weight materials with high strength, stiffness and toughness for load-bearing applications like transportation and construction. Since it is challenging to achieve both high Young's modulus and toughness in man-made composites, many groups have turned to nature for inspiration.¹⁻⁵ In nature, the hierarchical structure of biological nanocomposites achieves the desired mechanical properties and complex biological functions in a synergistic manner.⁶ More specifically these biocomposites have a common design principle of hierarchical self-assembly of a high weight fraction of reinforcing nano-scaled domains promoting stiffness, and a small weight fraction of soft, organic domain enabling energy dissipation and suppressing catastrophic crack propagation.^{1, 7-9} A variety of biomimetic composites have been developed mimicking the brick-and-mortar structure of nacre with a layered assembly of high fraction of nanoplates, e.g. nanoclay or montmorillonite combined with a small amount of various soft polymers. Promising mechanical properties have been achieved, and there have been significant advances considering the composite preparation techniques; however, the focus has been on finding optimal mixing ratios, developing convenient up-scalable methods, or characterizing the composite structure.^{5, 10-15} Less attention has been paid to the interphase phenomena, although they are of pivotal importance for the control of the

structures and the final properties.^{9, 16} Previous conclusions regarding beneficial interactions between soft and hard domains are, at first sight, contradicting. On the one hand, the ionic attraction between oppositely charged components¹⁷ and, on the other hand, repulsion between like charges¹⁸ have been found beneficial. This paradox is most probably due to the very complex role of the soft domain. The toughening mechanism is a combination of interdomain slippage, reinforcement pull-out, weak links, sacrificial bonds and deformation of macromolecular conformations.¹⁹⁻²² Furthermore repulsive forces between components are especially important during composite formation, to ensure an evenly distributed structure, while some degree of attraction in dry state is essential for composite strength.

In addition to platelet-shaped inorganic reinforcement, Nature also includes numerous examples of fibrous reinforcing components, like fibroin in spider silk, and collagen in bone.¹ Nanofibrillated cellulose (NFC) has recently gained attention due to the unique mechanical properties of the cellulose crystal, including a high Young's modulus (in range of 140 GPa), high strength (few GPa) and low density.^{23, 24} But the natural abundance of this renewable, nontoxic material also plays a role because of the recent focus on sustainability. Quite strong films, or nanopapers, have been prepared from pure NFC,²⁵⁻²⁷ and thus, NFC is an attractive candidate for reinforcement of high-performance materials. In the absence of soft polymer, these materials are brittle, with low strain-to-failure values.²⁸⁻³¹

Whereas, if NFC is added as a minor reinforcing domain in a polymer matrix, the mechanical properties become a compromise between the properties of matrix and reinforcement, and the typical synergy of biomimetic materials cannot be achieved.³²⁻³⁴

However, as a major reinforcing component in biomimetic composites, NFC has recently shown potential.^{12, 17, 35} Despite the synergistic improvements of mechanical properties, the reported strength values are still far from what would be expected, considering the strength of the cellulose crystal.

Uniform dispersion of composite elements, unique interplay between the components interfaces, and hierarchical structure are critical and need to be well designed and understood in nanocomposites.^{36, 37} Yet, there is a lack of experimental studies of direct forces and nanoscaled-lubrication phenomena that might explain the role of these interactions for the mechanical properties of biomimetic composites. Fantner *et al.*³⁸ were able to show how sacrificial bonds and hidden length scales contribute to the toughening of bone in aqueous media by applying single molecule force spectroscopy. Raj *et al.*³⁹ studied the adhesion between polylactic acid (PLA) films and flax microbeads by colloidal probe microscopy, drawing conclusions relevant for flax/PLA composites. Adhesion experiments complemented with friction measurements, however, have not yet been accomplished for man-made composites.

Recently⁴⁰ we explored the interactions in aqueous media during composite formation between NFC and poly(ethyleneglycol) grafted carboxymethylated cellulose (CMC-g-PEG) and showed that there is an interconnection between aqueous lubrication and evenly distributed composite structure. However, no experimental evidence exists on the importance of nano-scaled lubrication between the components in dry state, despite the role of lubrication on toughness enhancement.

The aim of this work is to show the link between mechanical performance and the interactions at molecular level at the interfaces in biomimetic composites. For this purpose we chose NFC as the major reinforcing component and CMC-g-PEG as the soft dissipating polymer. In order to gain insight into the interactions at the fibril interfaces within the composite, the surface and friction forces between cellulose microspheres and NFC films were measured in air. By comparing symmetric systems, where both cellulose surfaces were covered with CMC-g-PEG, to asymmetric systems, where only one of the surfaces was covered, it was possible to understand the effect of CMC-g-PEG on the interactions at the fibril interfaces within the composite. The results are discussed in terms of the importance of boundary lubrication, origin of attraction between the components, and the possible existence of sacrificial bonds and fibril pullout. The nano-scaled interfacial interactions were further related to the mechanical properties of macroscopic composites and we speculate on how these interfacial phenomena contribute to crack propagation and toughening of composites.

Experimental section

Materials

Nanofibrillar cellulose (NFC) was prepared by fluidizing never-dried kraft hardwood birch pulps obtained from Finnish pulp mills. The pulp was washed to the sodium form according to Swerin *et al.*⁴¹ to control both the counter ion type and ionic

strength. The washed pulp was disintegrated through a high-pressure fluidizer (Microfluidics, M-110Y, Microfluidics Int. Co., Newton MA) for 6 passes. No chemical or enzymatic pretreatment was used prior to disintegration. The charge density of the pulp used was 0.065 meq/g and the zeta-potential of the corresponding NFC gel was -3 mV at pH 8.⁴²

All chemicals used were of analytical grade. Carboxymethyl cellulose (Na-CMC, 250 000 g/mol, DS 0.70, Sigma Aldrich), was dialyzed and freeze-dried prior to use. The charge density of dialyzed CMC was determined to be 3.6 mmol/g by direct polyelectrolyte titration⁴³ with 1,5-dimethyl-1,5-diazundecamethylene polymetho-bromide (8 kDa, 5.35 meq/g, Sigma Aldrich). CMC-g-PEG was prepared by reaction of CMC with methoxy polyethylene glycol amine (OMe-PEG-amine; 2kDa) in the presence of EDC and NHS as described before.⁴⁰

Methods

Preparation of NFC films NFC films were prepared by spin-coating aqueous NFC dispersions (1.2 g/L) onto muscovite mica substrates, following the procedure described by Ahola *et al.*⁴⁴ and slightly modified by Eronen *et al.*⁴² CMC-g-PEG was adsorbed on NFC films by depositing drops of 100 mg/L CMC-g-PEG solution at Ph 4.5 (50 mM acetic acid buffer) on NFC film. The polymer adsorption took place at room temperature overnight. After adsorption, the CMC-g-PEG/NFC samples were rinsed with deionized water and dried under nitrogen flow.

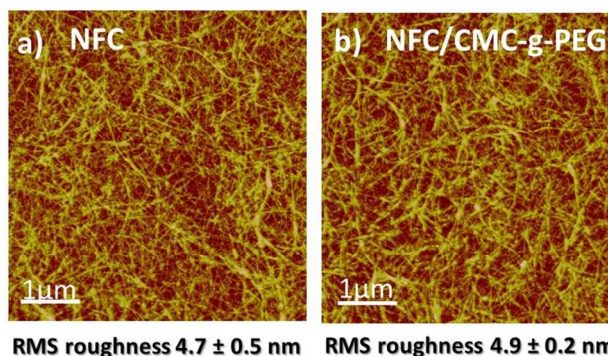


Fig.1 AFM images of NFC films before (a) and after (b) CMC-g-PEG adsorption. Scale bar: 1 μ m; vertical z-scale: 18 nm.

Atomic force microscopy The NFC films deposited on mica substrates were characterized by atomic force microscopy using a MultiMode AFM with a Nanoscope V controller (Bruker Corporation, Massachusetts, USA). Images of NFC films before and after CMC-g-PEG adsorption were obtained in air using silicon NSC15/AIBS cantilevers (MicroMasch, Tallinn, Estonia) with a tip radius below 10 nm, operating in tapping mode. Research NanoScope 8.15 software (Bruker Corporation) was used for image analysis. The only image processing applied was flattening. The RMS roughness of the NFC films was calculated from images of 25 μ m² area. Average RMS values from at least 6 different spots on the same or identically-prepared samples were 4.7 \pm 0.5 nm and 4.9 \pm 0.2 nm for NFC films before and after CMC-g-PEG adsorption, respectively (Fig. 1).

Friction and force measurements The surface and friction forces between NFC films and spherical microparticles of

amorphous cellulose were measured using the colloidal probe technique (CPM).⁴⁵ The colloidal probes were prepared by gluing cellulose spheres with diameters in the range of 15-20 μm (determined with a Leica DM750 optical microscope) at the end of tipless CSC12 cantilevers (MikroMasch) with the help of a micromanipulator (Narishige, Japan). An optical adhesive (Norland Products Inc., Cranbury, USA), cured under UV light, was used in the preparation of the cellulose colloidal probes. Force and friction experiments were carried out with the above mentioned AFM equipped with a closed-loop PicoForce scanner, following the procedures described by Ralston *et al.*⁴⁶ Briefly, during normal force measurements the cellulose colloidal probe approached the NFC substrate at a speed of 1 $\mu\text{m/s}$ until contact, and then separated. The surface forces obtained from the vertical deflection of the cantilever and the cantilever normal spring constant were normalized by the radius R of the cellulose sphere used as a colloidal probe. In friction force measurements, the cellulose colloidal probe slid over the NFC film at a speed of 10 $\mu\text{m/s}$ at different applied (compressive) loads. The friction forces were obtained from the lateral twist of the cantilever and the cantilever lateral spring constant. Before gluing the cellulose microparticles, the spring constants of the cantilevers were determined from the analysis of the cantilever thermal vibrations with the software AFM Tune IT v2.5 (ForceIT, Sweden) and the use of Sader's equations.^{47, 48} Values of about 0.25 N/m and 1.9×10^{-9} Nm/rad were obtained for the normal and lateral spring constants, respectively. CMC-g-PEG was adsorbed either on NFC film, on the cellulose colloidal probe or on both, from 100 mg/L polymer solution at pH 4.5 overnight, followed by rinsing with deionized water and drying under nitrogen flow. Subsequent force and friction measurements were performed at room temperature and at 35% relative humidity (RH). The humidity was controlled with a home-made humidity chamber, inside which a sample of MgCl_2 saturated solution was placed. RH inside the humidity chamber was monitored with a HM34C humidity probe (Vaisala, Vantaa, Finland).

Nanocomposite film preparation: To a 0.84% NFC water suspension 1% w/w of CMC-g-PEG and 10 ml acetic acid buffer solution was added. The pH was set to 4.5 with 0.1 M HCl. The dispersion was stirred overnight whereupon free-standing nanocomposite films were prepared by pressurized filtration and hot pressing for two hours as described previously.²⁷

Tensile tests were carried out with an Instron 4204 universal tensile testing machine and Bluehill 2 program. The gauge length, load cell and crosshead speed were 30 mm, 100 N, and 0.5 mm min^{-1} , respectively. A minimum of five specimens were measured from each sample. The thickness of each specimen was measured before the experiments and was 0.055-0.06 mm for NFC and 0.062-0.064 mm for NFC/CMC-g-PEG. The films were conditioned for seven days in ambient atmosphere at 23 $^{\circ}\text{C}$ and 40 - 50 % relative humidity prior to measurements. Film specimens of 5.30 mm width were cut from NFC film sheets with a pair of scissors. The specimens ($\sim 50 \text{ mm} \times 5.30 \text{ mm}$) were secured to rectangular paper strips from both ends using cyanoacrylate superglue (Loctite). The specimens' shape and dimensions are presented on Fig. 2.

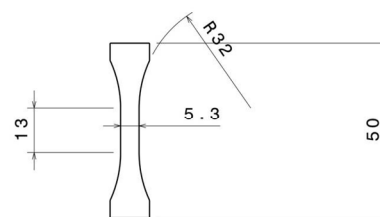


Fig.2 Dog-bone geometry of specimens used in the tensile testing. The units are in millimeters.

It is important to notice that the specimen shape was different to the previously used rectangular shape.²⁷ The dog bone shape facilitated less scatter in the results and failure always occurred at the gauge section, not at the grip, so direct comparison to results for other sample shapes should be avoided.

Results and discussion

The effect of CMC-g-PEG adsorption on normal and friction forces between cellulose surfaces.

Recently we found that CMC-g-PEG has a very strong lubricating effect on NFC in aqueous media. By small addition of such modified polysaccharide, the friction coefficient between the NFC film and the amorphous cellulose sphere in CPM decreased up to 88%.⁴⁰ Such a notable reduction was mainly due to double layer repulsion and weakly overlapping highly hydrated polymer chains. That efficient aqueous lubrication led to the formation of uniform composites without aggregates. It has been suggested that frictional sliding between load bearing components in nanocomposites is important for efficient energy dissipation in the toughening mechanism of the material.⁴⁹ Sacrificial bond rupture has also been found to be able to dissipate enormous amounts of energy, leaving the structural integrity intact.²¹ A detailed analysis of the interfacial forces and the friction at the nanoscale between the components of a composite material based on NFC and CMC-g-PEG is presented in this work. The results are related to the mechanical properties of free-standing composites in air.

Fig. 3a shows a typical force curve for the interaction between a spherical microparticle of amorphous cellulose and a NFC film deposited on a mica substrate. An attractive force was observed at short separation, causing the cellulose surfaces to jump into contact (inset of Fig. 3a). High adhesion was detected when the cellulose surfaces were subsequently separated (Fig. 3a). Attractive van der Waals forces and the formation of hydrogen bonds are probably the origin of that high adhesion.

Fig. 3b presents the friction force between these cellulose surfaces (cellulose colloid probe and NFC film) as a function of applied load. Once the surfaces reached contact, the friction force increased linearly with the applied load (load curve) as predicted by Amontons' law:

$$F_{\text{Friction}} = \mu F_{\text{Load}} \quad (1)$$

where μ is the friction coefficient. In systems with high adhesion between the surfaces, the adhesive forces contribute significantly to the total applied load. In those systems, the friction force is not

zero when the external applied load vanishes, because the adhesive forces keep the surfaces in contact with an effective load. Consequently, Amontons' law has to be modified to consider a finite value of friction F_0 when the external applied load F_{Load} is zero:

$$F_{Friction} = \mu F_{Load} + F_0 \quad (2),$$

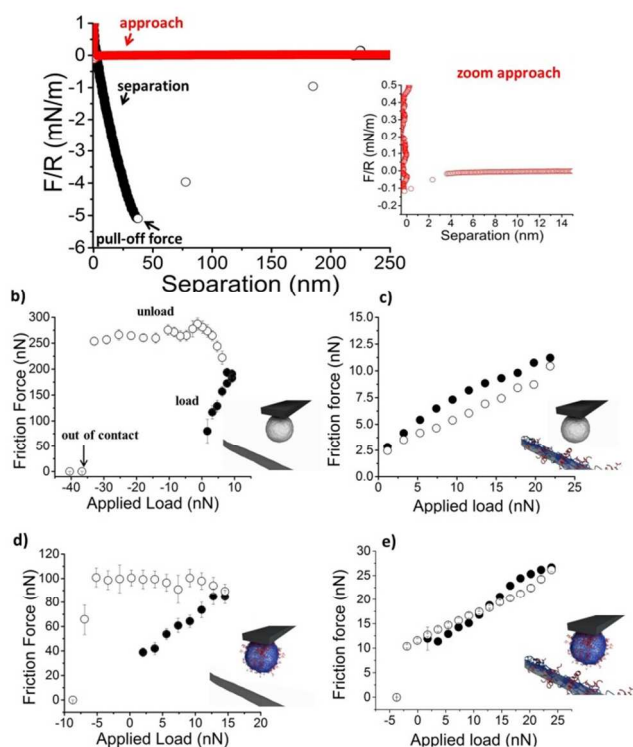


Fig.3 a) The normal force curves for the interaction between a cellulose colloidal probe and an NFC film on approach (red) and separation (black). The inset shows a zoom of the approach curve. b) Friction force between a cellulose colloidal probe and a NFC film as a function of applied load. c-e) Friction force between a cellulose colloidal probe and a NFC film as a function of applied load after adsorption of CMC-g-PEG on: c) only NFC film; d) only cellulose colloidal probe; and e) both on NFC film and cellulose colloidal probe. Closed symbols in (b-e) correspond to load curves, whereas open symbols represent retract curves. All measurements were performed at 35% RH.

The load curve in Fig. 3b follows the linear relation described by equation (2), and the friction coefficient can be obtained from the slope of the line that fits the experimental data (Table 1). At an external applied load of about 10 nN the loading cycle was reversed and the friction force was measured as the load is stepwise reduced (open symbols in Fig. 3b). A significant hysteresis was observed. Friction hysteresis has been previously observed in cellulosic systems and were ascribed to an increase in true contact area^{50, 51} or capillary condensation.⁵² It has been reported that the effect of capillary condensation on the adhesion and friction hysteresis between cellulose surfaces is especially pronounced at RH above 60%.⁵² In this work force and friction measurements were carried out at 35% RH, well below the indicated threshold of 60% for the formation of capillary condensates. Friction experiments carried out at 8% RH exhibited friction hysteresis similar to the one presented in Fig. 3b (results not shown), which discards capillary condensation as the main cause of the friction hysteresis in our system. A very interesting

feature in Fig. 3b is the remarkable increase of the friction force when the applied load started to be reduced from the maximum value of about 10 nN. Considering the high adhesion observed between the cellulose sphere and the NFC film (Fig. 3a), probably some NFC fibrils were partly pulled out when the separation of the surfaces was initiated by gradually decreasing the applied load. The partly pulled out NFC fibrils would alter the roughness and the contact area at the contact spot between cellulose sphere and NFC film, explaining the initial increase of the friction force in the unload curve and the subsequent hysteresis. As a consequence of the high adhesion in this system, negative applied loads beyond -30 nN were necessary to finally separate the cellulose surfaces (out of contact in Fig. 3b).

Figures 3c-e show the friction curves between a cellulose colloidal probe and a NFC film when CMC-g-PEG was adsorbed on one or both surfaces. In general, CMC-g-PEG had a lubrication effect since lower friction values were observed after polymer adsorption. For instance, the friction force of 165 nN between cellulose sphere and NFC film at an applied load of 10 nN was reduced to 65 nN, 7.5 nN or 15 nN when CMC-g-PEG was adsorbed on the cellulose sphere, on the NFC film or on both surfaces, respectively. The friction hysteresis observed between uncoated cellulose surfaces vanished after CMC-g-PEG adsorption on NFC film (Figs. 3c, e). Although of lower magnitude, friction hysteresis was still present between pure NFC fibrils and CMC-g-PEG coated cellulose sphere (Fig. 3d). These results suggest that the uncoated NFC films are responsible for the friction hysteresis, supporting the hypothesis that pulling out of NFC fibrils is the underlying mechanism of that phenomenon.

The friction data can be associated with the strength of the adhesion between the surfaces, quantified from the pull-off forces in the separation force curves (Figs. 3a and 4b). Table 1 presents the average values of pull-off forces for the different cellulose systems studied in this work. The high adhesion observed between cellulose sphere and NFC film (-6.3 ± 1.4 mN/m) was dramatically reduced when NFC was coated with CMC-g-PEG (Table 1 and Fig. 4b). PEG chains hinder the formation of hydrogen bonds between the cellulose surfaces, considerably diminishing the contribution of those bonds to the total adhesion. The adhesion in the system cellulose sphere vs. NFC coated with CMC-g-PEG (-0.8 ± 0.3 mN/m) was too low to provoke a significant pulling out of the NFC fibrils and, therefore, no friction hysteresis was observed in Fig. 3c. Intermediate values of pull-off forces (-2.8 ± 0.08 mN/m) were obtained when CMC-g-PEG was adsorbed only on the cellulose sphere. The high affinity of CMC to NFC partly compensates for the hindering effect of PEG chains on the formation of hydrogen bonds. As a consequence, the adhesion in that system was strong enough to cause some pulling out of NFC fibrils, giving rise to the friction hysteresis observed in Fig. 3d. In comparison with Fig. 3b, the intensity of the friction hysteresis was substantially smaller because the adhesion was also lower in that system. Finally, a moderate adhesion (-2.4 ± 1.1 mN/m) was also observed when both surfaces were coated with CMC-g-PEG, significantly higher than in the asymmetrical system where CMC-g-PEG were adsorbed only on NFC film. The higher adhesion observed in the former system could be due to the entanglement of PEG chains

from both surfaces. In spite of the higher adhesion, no friction hysteresis was observed in this system (Fig. 3e), which seems to point that NFC fibrils coated with CMC-g-PEG were less prone to be pulled out.

Table 1. Pull-off forces and friction coefficients between different cellulose surfaces. Mean values of at least 6 (pull-off forces) and 3 (friction coefficients) measurements are presented together with their standard deviations.

System	Pull-off forces (mN/m)	friction coefficients
Cellulose sphere vs. NFC	-6.3 ± 1.4	8.44 ± 2.58
Cellulose sphere vs. NFC/CMC-g-PEG	-0.8 ± 0.3	0.57 ± 0.07
Cellulose sphere /CMC-g-PEG vs. NFC	-2.8 ± 0.8	3.97 ± 0.23
Cellulose sphere /CMC-g-PEG vs. NFC /CMC-g-PEG	-2.4 ± 1.1	0.83 ± 0.20

Table 1 also presents the friction coefficients for different cellulose systems, calculated from the linear fits of the friction data corresponding to the load curves in Figs. 3b-e. The lubrication effect of CMC-g-PEG is reflected in the lower values of the friction coefficient obtained when the polymer was adsorbed on one or both cellulose surfaces. The friction coefficient between the cellulose sphere and the NFC film decreased one order of magnitude (from 8.44 ± 2.58 to 0.57 ± 0.07) after the adsorption of CMC-g-PEG on NFC. Since polymer adsorption did not alter the RMS roughness of the NFC substrates (Fig. 1), the reduction cannot be explained by a difference in roughness.^{53, 54} The important reduction in the friction coefficient must be related to the dramatic decrease of adhesion observed after coating the NFC with CMC-g-PEG, and the consequent effect on the partial pulling out of NFC fibrils, as pointed out before. The intermediate value of 3.97 ± 0.23 for the friction coefficient between the NFC film and the cellulose sphere modified with CMC-g-PEG correlates with the intermediate adhesion and friction hysteresis in that system. A low friction coefficient of 0.83 ± 0.20 was obtained when the polymer was adsorbed on both surfaces. Still, the adhesion in this system was of similar magnitude as when only the cellulose sphere was coated with CMC-g-PEG. Nevertheless, the friction coefficient when both surfaces were coated by CMC-g-PEG is slightly higher than in the case where the polymer was only adsorbed on NFC (0.83 ± 0.20 vs. 0.57 ± 0.07), which could be probably due to the entanglement of PEG chains from both surfaces.

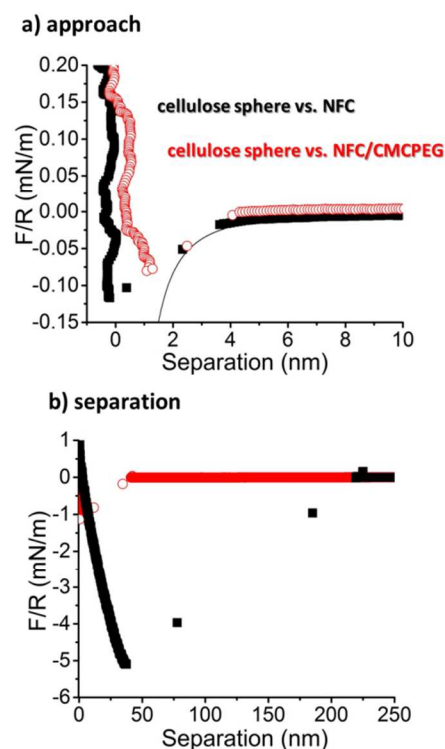


Fig. 4 Normal force curves on approach (a) and separation (b) for the interaction between a cellulose sphere and a NFC film without (black closed symbols) and with (red open symbols) CMC-g-PEG coating. The solid line in panel a) represents the theoretical fit according to equation (3) for van der Waals attraction, using a Hamaker constant of 0.2×10^{-20} J.

Fig. 4 shows two characteristic normal force curves for the interaction of a cellulose sphere with an unmodified NFC film and with NFC modified by CMC-g-PEG adsorption. Similar attractions at short separation distances were observed in both systems when approaching the surfaces (Fig. 4a). That attraction eventually provoked the surfaces to jump into contact from distances within the range 4-7 nm. Similar attractive forces were observed when the cellulose sphere was coated with CMC-g-PEG (Fig. S1 Supplementary information). Considering the conditions chosen to carry out the force experiments (in air, RH 35%), the attraction observed at short distances must be due to van der Waals forces, which can be described by Equation (3) for the case of interaction between a flat surface and a sphere of radius R ,

$$\frac{F_{vdW}}{R} = -\frac{A}{6x^2} \quad (3),$$

where A is the Hamaker constant of the system and x is the separation between the surfaces. Using a Hamaker constant of 0.2×10^{-20} J, equation (3) fits the experimental data very well (solid line in Fig. 4a). At distances below 2 nm, when the gradient of the attractive force exceeded the spring constant of the cantilever, the surfaces jumped directly into contact. The Hamaker constant of 0.2×10^{-20} J used in this study for cellulose surfaces interacting in air is about 30 times lower than the value of 5.8×10^{-20} J previously reported by Bergström *et al.*⁵⁵ from spectroscopic ellipsometry experiments. However, it must be taken into account that their results were obtained with very smooth regenerated cellulose films with an RMS roughness in the

range 0.16-0.24 nm. The NFC films used in this work were considerably rougher with an RMS roughness of 4-5 nm (Fig. 1). Van der Waals forces are affected by surface roughness, decreasing as the roughness increases.⁵⁶ The effect of roughness in equation (3) is reflected in a lower effective Hamaker constant.

The Mechanical properties of free standing films

The nanoscaled interactions between components discussed above were further linked to the macroscopic properties of the composites. We focused on demonstrating the connection between adhesion and lubrication on mechanical performance, not on finding optimal ratios between components. Thus, only one ratio of components was studied. Although there is some removal of fibrils during film formation,²⁷ the low concentration of CMC-g-PEG (1 w/w %) ensures that all added polymer is adsorbed to the fibrils and the ratio will be unaffected by the filtration. About 2 w-% of CMC can irreversibly adsorb to cellulose fibers depending on the polymer charge⁵⁷ but adsorption on NFC could be higher due to larger accessible surface area. In a recent study by Pahimanolis *et al.*,¹⁸ increasing the CMC concentration in NFC/CMC composites above 5% did not improve the mechanical properties of a composite film prepared by tape casting. Lower concentrations were not tested. We speculate that at higher CMC content a non-adsorbed polymer layer will not take part in enhancing the mechanical properties because these molecules are not interacting with NFC.

In Fig.5 the stress-strain curve for pure NFC film and NFC/CMC-g-PEG nanocomposite are compared and in Table 2 the corresponding Young's modulus, stress, and strain-to-break values for these samples are listed.

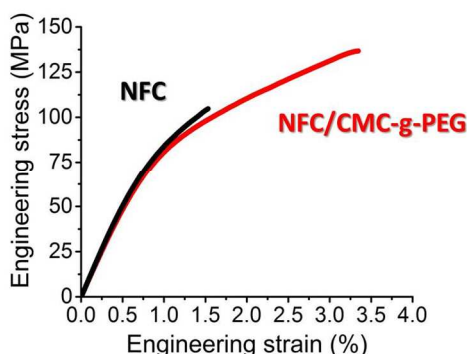


Fig.5 Stress-strain curves for NFC/CMC-g-PEG composite (red) and 100% NFC reference (black)

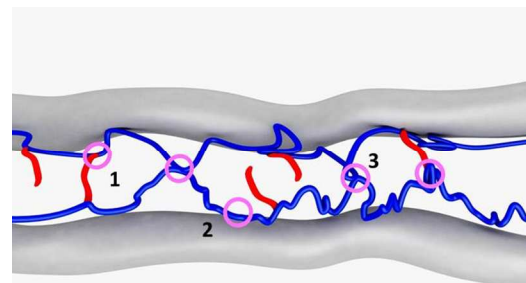
Table 2. Tensile Properties of films

Sample	Young's Modulus (GPa)	Engineering stress (MPa)	Strain-to-failure (%)	Work-of-fracture (MJ/m ³)
NFC (100%)	10.39 ± 0.14	107.11 ± 1.64	1.5 ± 0.09	1.04
NFC/CMC-g-PEG (99/1 %)	9.49 ± 0.48	124.42 ± 7.60	2.7 ± 0.56	3.09

For pure NFC nanopaper the Young's modulus can reach a value

of 10.4 GPa. Upon a small addition of CMC-g-PEG the modulus only slightly decreases to the value 9.5 GPa. However, the stress-strain curve is different, indicating different interactions between the components other than those between pure nanofibrils. After addition of a small amount of CMC-g-PEG more plastic deformation is observed. The work-of-fracture, estimated by the area under the stress-strain curve,²⁵ was almost three times higher for the nanocomposite than for unmodified NFC paper. The work-of-fracture is a measure of material toughness, and the increased toughness also allows reaching higher engineering strength, as observed in Fig 5. We speculate that the observed synergy is related to the surface forces between the components and to the complex role of the soft polysaccharide layer.

Evans *et al.*^{58, 59} suggested that the lubricating effect of the soft domains in nacre leads to shearing and stretching of the organic phase within the slipping reinforcing domains, and provides resistance to deformation. We suggest that the CMC-g-PEG phase works in a similar way in the NFC/CMC-g-PEG nanocomposite, as shown by the low friction. Furthermore, the strong adhesion present at both the NFC vs. CMC-g-PEG interface, and when both cellulose surfaces are modified with CMC-g-PEG, (see Table 1) ensures good bonding. Additionally, hydrogen bond formation and their rupture (Scheme 1) during the sliding, when load is applied, could further contribute to toughening.



Scheme 1. Possible kinds of weak bonds (hydrogen bonds and van der Waals attraction) between NFC and CMC-g-PEG interfaces involving in gluing the fibrils together, (1) between PEG and CMC, (2) between CMC and NFC, and (3) between CMC from one chain with CMC from other chain.

The presence of hydrogen bonds also facilitates sacrificial bonds and stretching of hidden length as has previously been reported during deformation of wood,⁶⁰ or in mineralized collagen fibers.³⁸ The stick-slip mechanism, observed in friction force experiments could provide, and explain, the plastic response observed during deformation. We also speculate that partial fibril pullout and intermixing of phases may enable more effective crack deflection at the hard/soft (NFC/CMC-g-PEG) interface, converting the brittle NFC into a more ductile material. However, we acknowledge that we can only speculate at the moment and more careful examination of fraction regime and the crack dissipation mechanism would be needed.

Finally, the lubrication in liquid state⁴⁰ and the improved dispersibility between modified NFC fibrils obviously benefit the formation of a more uniform composite and, as a consequence, improved mechanical properties.

Conclusions

We have employed a simple, novel and versatile concept to conjugate nanofibrillated cellulose with soft polymers by non-ionic interactions. This allows creating a biomimetic nanocomposite that contains a large ratio of reinforcing NFC fibrils separated by thin layers of soft polymer. CMC was used as a binding agent to introduce, via non-ionic interactions, soft polymers (PEG) to the fibrils, and design the composite with hierarchically ordered soft/hard architecture. The clear increase in material toughness in the presence of CMC-g-PEG was linked to experimental verification of the interactions between the components by employing colloidal probe microscopy. The weak multiple hydrogen bonds, intermixing of phases and decrease in friction observed at molecular level contribute to the complex energy dissipation mechanism during fracture of composites and leads to enhanced toughness. Direct measurement of the interfacial forces give information otherwise not available that enhance our understanding of nanocomposite behaviour. Since CMC can be widely functionalized with different molecular architectures and constituents, we expect numerous possibilities to follow up this concept in order to design biomimetic nanocomposites based on polysaccharide modification, where increased fracture toughness as well as high stiffness and strength of reinforcing NFC components can be achieved. Further studies related to polysaccharide modification and their role in toughening mechanism are currently being conducted.

Acknowledgments

Mechanical test were performed with help of Arto Salminen at the Department of Polymer Chemistry (Aalto University). Prof. Mark Rutland (KTH) is acknowledged for providing the cellulose spheres. Maciej Elert is thanked for the illustration. AO would like to gratefully acknowledge M. Kanerva for fruitful discussions of mechanical testing. Dr. Joseph Campbell is thanked for the linguistic revision of the manuscript. Funding for this work was received from Naseva-project supported by Finnish Technology Development Centre (TEKES) and industrial partners.

Notes and references

⁴⁰ Aalto University School of Chemical Technology: Department of Forest Product Technology; E-mail: anna.olszewska@aalto.fi; monika.osterberg@aalto.fi

⁴⁵ † Electronic Supplementary Information (ESI) available: [Fig. S1 Normal force on approach and separation where the cellulose sphere modified with CMC-g-PEG interacts with NFC and NFC/CMC-g-PEG films]. See DOI: 10.1039/b000000x/

References

- ¹ M. A. Meyers, P. Chen, A. Y. Lin and Y. Seki, *Progress in Materials Science*, 2008, **53**, 1-206.
- ² E. Munch, M. E. Launey, D. H. Alsem, E. Saiz, A. P. Tomsia and R. O. Ritchie, *Science*, 2008, **322**, 1516-1520.
- ³ L. J. Bonderer, A. R. Studart and L. J. Gauckler, *Science*, 2008, **319**, 1069-1073.
- ⁴ A. Walther, I. Bjurhager, J. - Malho, J. Pere, J. Ruokolainen, L. A. Berglund and O. Ikkala, *Nano Letters*, 2010, **10**, 2742-2748.

- ⁵ P. Das, S. Schipmann, J. Melho, B. Zhu, U. Klemradt and A. Walther, *ACS Applied Materials & Interfaces*, 2013, **5**, 3738-3747.
- ⁶ E. Manias, *Nature Materials*, 2007, **6**, 9-11.
- ⁷ H. Peterlik, P. Roschger, K. Klaushofer and P. Fratzl, *Nature Materials*, 2006, **5**, 52-54.
- ⁸ P. Fratzl, H. S. Gupta, F. D. Fischer and O. Kolednik, *Advanced Materials*, 2007, **19**, 2657-2661.
- ⁹ P. Fratzl and R. Weinkamer, *Progress in Materials Science*, 2007, **52**, 1263-1334.
- ¹⁰ A. J. Svagan, M. A. S. Azizi Samir and L. A. Berglund, *Biomacromolecules*, 2007, **8**, 2556-2563.
- ¹¹ A. J. Svagan, M. A. S. Azizi Samir and L. A. Berglund, *Advanced Materials*, 2008, **20**, 1263-1269.
- ¹² M. Wang, A. Olszewska, A. Walther, J. Malho, F. H. Schacher, J. Ruokolainen, M. Ankerfors, J. Laine, L. A. Berglund, M. Österberg and O. Ikkala, *Biomacromolecules*, 2011, **12**, 2074-2081.
- ¹³ A. Liu, A. Walther, O. Ikkala, L. Belova and L. A. Berglund, *Biomacromolecules*, 2011, **12**, 633-641.
- ¹⁴ P. Laaksonen, A. Walther, J. Malho, M. Kainlauri, O. Ikkala and M. B. Linder, *Angewandte Chemie International Edition*, 2011, **50**, 8688-8691.
- ¹⁵ A. Liu and L. A. Berglund, *European Polymer Journal*, 2013, **49**, 940-949.
- ¹⁶ J. Jancar, *Journal of Materials Science*, 2008, **43**, 6747-6757.
- ¹⁷ H. Jin, A. Cao, E. Shi, J. Seitsonen, L. Zhang, R. H. Ras, L. A. Berglund, M. Ankerfors, A. Walther and O. Ikkala, *Journal of Materials Chemistry B*, 2013, **1**, 835-840.
- ¹⁸ N. Pahimanolis, A. Salminen, P. A. Penttilä, J. T. Korhonen, L. Johansson, J. Ruokolainen, R. Serimaa and J. Seppälä, *Cellulose*, 2013, **20**, 1459-1468.
- ¹⁹ M. J. Buehler, *Proceedings of the National Academy of Sciences*, 2006, **103**, 12285-12290.
- ²⁰ M. E. Launey, M. J. Buehler and R. O. Ritchie, *Annual Review of Material Research*, 2010, **40**, 25-53.
- ²¹ M. J. Palmeri, K. W. Putz and L. C. Brinson, *ACS Nano*, 2010, **4**, 4256-4264.
- ²² D. Sen and M. J. Buehler, *Scientific Reports*, 2011, **1**, 1-35.
- ²³ S. Iwamoto, W. Kai, A. Isogai and T. Iwata, *Biomacromolecules*, 2009, **10**, 2571-2576.
- ²⁴ H. Yano, J. Sugiyama, A. Nakagaito, M. Nogi, T. Matsuura, M. Hikita and K. Handa, *Advanced Materials*, 2005, **17**, 153-155.
- ²⁵ M. Henriksson, L. A. Berglund, P. Isaksson, T. Lindström and T. Nishino, *Biomacromolecules*, 2008, **9**, 1579-1585.
- ²⁶ H. Sehaqui, Q. Zhou, O. Ikkala and L. A. Berglund, *Biomacromolecules*, 2011, **12**, 3638-3644.
- ²⁷ M. Österberg, J. Vartiainen, J. Lucenius, U. Hippel, K. Seppälä, R. Serimaa and J. Laine, *ACS Applied Materials & Interfaces*, 2013, **5**, 4640-4647.
- ²⁸ A. N. Nakagaito and H. Yano, *Cellulose*, 2008, **15**, 555-559.
- ²⁹ A. N. Nakagaito and H. Yano, *Cellulose*, 2008, **15**, 323-331.
- ³⁰ K. Syverud and P. Stenius, *Cellulose*, 2009, **16**, 75-85.
- ³¹ H. Fukuzumi, T. Saito, T. Iwata, Y. Kumamoto and A. Isogai, *Biomacromolecules*, 2009, **10**, 162-165.
- ³² T. Zimmermann, E. Pöhler and T. Geiger, *Advanced Engineering Materials*, 2004, **6**, 754-761.
- ³³ T. Zimmermann, E. Pöhler and P. Schwaller, *Advanced Engineering Materials*, 2005, **7**, 1156-1161.
- ³⁴ M. Bulota, K. Kreitsmann, M. Hughes and J. Paltakari, *J Appl Polym Sci*, 2012, **126**, E449-E458.
- ³⁵ A. Walther, J. V. I. Timonen, I. Diez, A. Laukkanen and O. Ikkala, *Adv Mater*, 2011, **23**, 2924-2928.
- ³⁶ B. Pukanszky, *European Polymer Journal*, 2005, **41**, 645-662.
- ³⁷ N. D. Wanasekara and L. T. J. Korley, *Journal of Polymer Science, Part B: Polymer Physics*, 2013, **51**, 463-467.
- ³⁸ G. Fantner, T. Hassenkam, J. H. Kindt, J. C. Weaver, H. Birkedal, L. Pechenik, J. A. Cutoroni, G. A. G. Cidade, G. D. Stucky, D. E. Morse and P. K. Hansma, *Nature Materials*, 2005, **4**, 612-616.
- ³⁹ G. Raj, E. Balnois, C. Baley and Y. Grohens, *Colloids and Surfaces A: Physicochemical and Engineering Aspects*, 2009, **352**, 47-55.
- ⁴⁰ A. Olszewska, K. Junka, N. Nordgren, J. Laine, M. W. Rutland and M. Österberg, *Soft Matter*, 2013, **9**, 7448-7457.

- 41 A. Swerin, L. Ödberg and T. Lindström, *Nordic Pulp and Paper Research Journal*, 1990, **5**, 188-196.
- 42 P. Eronen, J. Laine, J. Ruokolainen and M. Österberg, *J. Colloid Interface Sci.*, 2012, **373**, 84-93.
- 5 43 L. Winter, L. Wågberg, L. Ödberg and T. Lindström, *Journal of Colloid and Interface Science*, 1986, **111**, 537-543.
- 44 S. Ahola, J. Salmi, L. Johansson, J. Laine and M. Österberg, *Biomacromolecules*, 2008, **9**, 1273-1282.
- 45 Ducker W A, Senden T.J. and Pashley R.M., *Nature*, 1991, **353**, 239-241.
- 10 46 J. Ralston, I. Larson, M. W. Rutland, A. A. Feiler and M. Kleijn, *Pure Applied Chemistry*, 2005, **77**, 2149-2170.
- 47 C. Green, H. Lioe, J. Cleveland, R. Proksch, P. Mulvaney and J. Sader, *Rev. Sci. Instrum.*, 2004, **75**, 1988-1996.
- 15 48 J. Sader, J. Chon and P. Mulvaney, *Rev. Sci. Instrum.*, 1999, **70**, 3967-3969.
- 49 M. C. Larson and H. F. Miles, *Mechanics of Materials*, 1998, **27**, 77-89.
- 50 Y. L. Chen, C. A. Helm and J. N. Israelachvili, *Journal of Physical Chemistry B*, 1991, **95**, 10736-10747.
- 20 51 G. Bogdanovic, F. Tiberg and M. W. Rutland, *Langmuir*, 2001, **17**, 5911-5916.
- 52 A. Feiler, J. Stiernstedt, K. Theander, P. Jenkins and M. W. Rutland, *Langmuir*, 2007, **23**, 517-522.
- 25 53 M. A. Plunkett, A. Feiler and M. W. Rutland, *Langmuir*, 2003, **19**, 4180-4187.
- 54 A. Feiler, P. Jenkins and M. W. Rutland, *Journal of Adhesion Science and Technology*, 2005, **19**, 165-179.
- 55 L. Bergström, S. Stemme, T. Dahlfors, H. Arwin and L. Ödberg, *Cellulose*, 1999, **6**, 1-13.
- 30 56 P. Mazur and A. A. Maradudin, *Physical Review B*, 1981, **23**, 695-705.
- 57 J. Laine, T. Lindstrom, G. Glad Nordmark and G. Risinger, *Nord. Pulp Pap. Res. J.*, 2000, **15**, 520-526, Paper and coating chemistry symposium, Stockholm, Sweden, 6-8 June 2000 (C, K, P, S).
- 35 58 R. Z. Wang, Z. Suo, A. G. Evans, N. Yao and I. A. Aksay, *Journal of Material Research*, 2001, **16**, 2485-2493.
- 59 A. G. Evans, Z. Suo, R. Z. Wang, I. A. Aksay, M. Y. He and J. W. Hutchinson, *Journal of Material Research*, 2001, **16**, 2475-2484.
- 60 J. Keckes, I. Burgert, K. Frühmann, M. Müller, K. Kölln, M. Hamilton, M. Burghammer, S. V. Roth, S. Stanzl-Tschegg and P. Fratzl, *Nature Materials*, 2003, **2**, 810-814.
- 40

We utilized colloidal probe microscopy to study the nano-scaled interfacial interactions, which can be further related to the mechanical properties of macroscopic composites.

